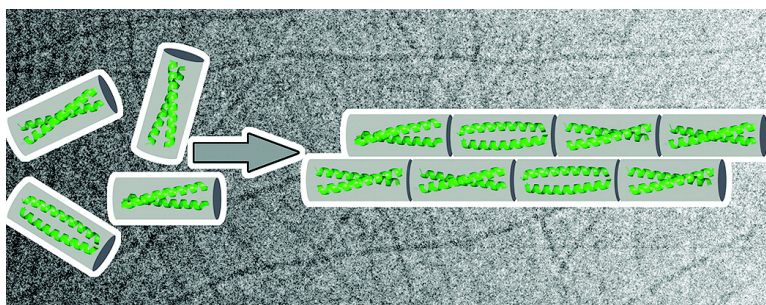


Self-Assembly of β -Helical Coiled Coil Nanofibers

He Dong, Sergey E. Paramonov, and Jeffrey D. Hartgerink

J. Am. Chem. Soc., **2008**, 130 (41), 13691-13695 • DOI: 10.1021/ja8037323 • Publication Date (Web): 20 September 2008

Downloaded from <http://pubs.acs.org> on February 8, 2009



More About This Article

Additional resources and features associated with this article are available within the HTML version:

- Supporting Information
- Access to high resolution figures
- Links to articles and content related to this article
- Copyright permission to reproduce figures and/or text from this article

[View the Full Text HTML](#)

Self-Assembly of α -Helical Coiled Coil Nanofibers

He Dong, Sergey E. Paramonov, and Jeffrey D. Hartgerink*

Department of Chemistry and Department of Bioengineering, Rice University,
6100 Main Street, Mail Stop 60, Houston, Texas 77005

Received May 19, 2008; E-mail: jdh@rice.edu

Abstract: The α -helical coiled coil is one of the best-studied and most well-understood protein folding motifs. In particular, the coiled coil can be made to self-assemble into a nanofibrous architecture with many potential applications in biomimetic engineering and elsewhere. The key to the assembly of such nanofibers has been the formation of “sticky ended” dimers through careful selection of electrostatically charged amino acids. In this work, we demonstrate for the first time that sticky ended dimers are not a prerequisite for α -helical coiled coil nanofiber formation. In contrast, we show that blunt-ended dimers are able to form nanofibers with a uniform diameter of 4 nm while being hundreds of nanometers in length. Furthermore, the length and lateral packing can be controlled through selection of amino acids not involved in the coiled coil interface.

Introduction

The coiled coil is a widely studied protein folding motif that is found in many natural proteins, including the transcription factor GCN4,¹ tropomyosin,^{2,3} myosin filaments,^{4–6} HIV virus coat protein⁷ and intermediate filaments.⁸ The coiled coil is one of the few motifs in which specific amino acid selection rules are able to predict peptide secondary structure and oligomerization state. It has been used as a structural motif for the formation of self-assembled fibers.^{9–12} Most notably, nanofibrous assembly has been demonstrated by Woolfson's group through carefully designed sticky ended propagation of self-assembly.¹⁰ The resulting structure can be tailored into different morphologies based on the composition of the building blocks. Examples of linear,^{10,13,14} kinked,¹⁵ waved,¹⁵ and branched

nanofibers¹⁶ have been demonstrated. Recently, this approach was used in combination with covalent capture to synthesize a polypeptide molecule with an estimated mass of ≥ 3 MDa.¹⁷ Although self-assembled fibrils have been successfully demonstrated by Woolfson's group and several others,^{12,18–20} an intricate design was required to form the necessary sticky ended dimers to promote the elongation of fibers. In this report, we demonstrate that coiled coil α -helical nanofibers can be formed through an alternative mechanism. We have found that coiled coil peptides without designed sticky ends will form nanofibers and that the fiber formation is highly concentration dependent. Control over fibril thickness can be engineered into the system through rational design of the peripheral amino acids in the *b*, *c*, and *f* positions of the heptad repeat to assemble elongated nanofiber with diameters as small as 4 nm. Although previous studies have reported the formation of thin coiled coil fibrils,^{18,21–23} our work combines an exceptionally small diameter with a rationally designed electrostatic control and a highly uniform fiber diameter. In this work, we demonstrate the formation of homogeneously thin coiled coil fibrils as characterized by transmission electron microscopy (TEM). Importantly, we use vitreous ice cryogenic TEM (cryo-TEM)

- (1) O'Shea, E. K.; Klemm, J. D.; Kim, P. S.; Alber, T. *Science* **1991**, *254*, 539–544.
- (2) McLachlan, A. D.; Stewart, M. *J. Mol. Biol.* **1975**, *98*, 293–304.
- (3) Hodges, R. S.; Sodek, J.; Smith, L. B.; Jurasek, L. *Cold Spring Harbor Symp. Quant. Biol.* **1972**, *37*, 299–310.
- (4) McLachlan, A. D.; Karn, J. *J. Mol. Biol.* **1963**, *164*, 605–626.
- (5) Rigotti, D. J.; Kokona, B.; Horne, T.; Acton, E. K.; Lederman, C. D.; Johnson, K. A.; Manning, R. S.; Kane, S. A.; Smith, W. F.; Fairman, R. *Anal. Biochem.* **2005**, *346*, 189–200.
- (6) Sinard, J. H.; Rimm, D. L.; Pollard, T. D. *J. Cell. Biol.* **1990**, *111*, 2417–2426.
- (7) Chan, D. C.; Fass, D.; Berger, J. M.; Kim, P. S. *Cell* **1997**, *89*, 263–273.
- (8) Herrmann, H.; Aebi, U. *Curr. Opin. Struct. Biol.* **1998**, *8*, 177–185.
- (9) Kojima, S.; Kuriki, Y.; Yoshida, T.; Yazaki, K.; Miura, K.-I. *Proc. Jpn. Acad. Ser. B: Phys. Biol. Sci.* **1997**, *73B*, 7–11.
- (10) Pandya, M. J.; Spooner, G. M.; Sunde, M.; Thorpe, J. R.; Rodger, A.; Woolfson, D. N. *Biochemistry* **2000**, *39*, 8728–8734.
- (11) Kajava, A. V.; Potekhin, S. A.; Corradin, G.; Leapman, R. D. *J. Pept. Sci.* **2004**, *10*, 291–297.
- (12) Potekhin, S. A.; Melnik, T. N.; Popov, V.; Lanina, N. F.; Vazina, A. A.; Rigler, P.; Verdini, A. S.; Corradin, G.; Kajava, A. V. *Chem. Biol.* **2001**, *8*, 1025–1032.
- (13) Smith, A. M.; Banwell, E. F.; Edwards, W. R.; Pandya, M. J.; Woolfson, D. N. *Adv. Funct. Mater.* **2006**, *16*, 1022–1030.
- (14) Smith, A. M.; Acquah, S. F. A.; Bone, N.; Kroto, H. W.; Ryadnov, M. G.; Stevens, M. S. P.; Walton, D. R. M.; Woolfson, D. N. *Angew. Chem., Int. Ed.* **2005**, *44*, 325–328.

- (15) Ryadnov, M. G.; Woolfson, D. N. *Nat. Mater.* **2003**, *2*, 329–332.
- (16) Ryadnov, M. G.; Woolfson, D. N. *Angew. Chem., Int. Ed.* **2003**, *42*, 3021–3023.
- (17) Ryadnov, M. G.; Woolfson, D. N. *J. Am. Chem. Soc.* **2007**, *129*, 14074–14081.
- (18) Zimenkov, Y.; Dublin, S. N.; Ni, R.; Tu, R. S.; Breedveld, V.; Apkarian, R. P.; Conticello, V. P. *J. Am. Chem. Soc.* **2006**, *128*, 6770–6771.
- (19) Wagner, D. E.; Phillips, C. L.; Ali, W. M.; Nybakken, G. E.; Crawford, E. D.; Schwab, A. D.; Smith, W. F.; Fairman, R. *Proc. Natl. Acad. Sci. U.S.A.* **2005**, *102*, 12656–12661.
- (20) Zimenkov, Y.; Conticello, V. P.; Guo, L.; Thiyagarajan, P. *Tetrahedron* **2004**, *60*, 7237–7246.
- (21) Pagel, K.; Wagner, S. C.; Samedov, K.; Von Beripsch, H.; Boettcher, C.; Koksche, B. *J. Am. Chem. Soc.* **2006**, *128*, 2196–2197.
- (22) Dublin, S. N.; Conticello, V. P. *J. Am. Chem. Soc.* **2007**, *130*, 49–51.
- (23) Papapostolou, D.; Bromley, E. H. C.; Bano, C.; Woolfson, D. *J. Am. Chem. Soc.* **2008**, *130*, 5124–5130.

Table 1. Peptide Primary Sequences

#	<i>gabcdefgabcdefgabcdef</i>
1	EIKQLESEISKLEQEIQSLEK
2	EISQLESEISQLEQEIQSLES
3	EIAQLEYEISQLEQEIQALES
4	EIAQLEYEISQLEYEIQALES

to visualize the fiber morphology in its native hydrated state free from the artifacts induced by drying and staining.

A coiled coil peptide is an amphiphilic peptide characterized by a seven residue repeating unit, known as the *heptad* repeat. The amino acids involved in the repeat are denoted as *abcdefg*. The hydrophobic domain of the peptide is created by residues at the *a* and *d* positions, which appear together on the same side of the helix. Depending on the specifics of the design, two, three, four, or more peptides will self-assemble with one another in such a way as to exclude the hydrophobic residues from the aqueous environment. An ionic region is formed from amino acids at the *e* and *g* positions and can be used to modify and control the self-assembly driven through the hydrophobic region. For example, careful selection of amino acids in these positions allowed Woolfson's group to form a sticky ended nucleation point for fiber formation.^{10,24} Amino acids in the peripheral region (*b*, *c*, and *f* positions) have been less well studied but generally are required to be hydrophilic to enhance the peptide solubility in water and reduce the probability of α to β structural conversion.^{25,26}

In this paper, we described several coiled coil peptides that are differentiated by the amino acids in their peripheral region (*b*, *c*, and *f* positions). We show that when the peptide concentration is increased, three of the four peptides form nanofibers. With the incorporation of positively charged residues in the peripheral region, elongated nanofibers can be created and stabilized with narrow diameters of ~ 4 nm; however, without charge control, the self-assembly proceeds until matured fibers with diameters of 20 nm or more are reached. The observation of fibrils with a minimum diameter of ~ 4 nm instead of 2 nm, which is what one expects for a fiber formed from an individual coiled coil dimer, leads to an alternative mechanism of self-assembled coiled coil nanofiber formation. Additionally, the length of these nanofibers can also be engineered through the selection of amino acids with lower helix propensities.

Using the known rules governing coiled coil assembly,^{27,28} four peptides (Table 1) containing 21 amino acids each were synthesized.

These peptides share common primary structural features which include: (1) Positions *a* and *d* are filled with the amino acids isoleucine (I) and leucine (L), respectively, to form the hydrophobic patch. These particular hydrophobic amino acids were selected to favor the formation of a dimeric coiled coil. (2) Positions *e* and *g* are filled with glutamic acid (E) to provide a uniformly acidic ionic region. These also give us a molecular switch to control the assembly of the system based on a pH neutralization strategy. At low pH, ionic repulsion is eliminated

and carboxylic acid side chains may hydrogen bond with one another. (3) The key feature in the design to engineer the morphology of nanofibers is the selection of residues in the *b*, *c*, and *f* positions, which play a critical role in controlling the length and the diameter of peptide fibers and include lysine (K), glutamine (Q), serine (S), and tyrosine (Y).

Experimental Section

Peptide Synthesis and Purification. All peptides were synthesized following the general procedure for Fmoc-chemistry of solid phase peptide synthesis as previously described.^{25,26} The syntheses were carried out on an Apex-396 automatic peptide synthesizer based on a scale of 0.3 mmol. Peptide **1** was synthesized with a Wang resin whereas peptides **2–4** were prepared with Rink MBHA resin to give an amide terminated peptide at the C terminus. Peptides **2**, **3**, and **4** were acetylated in the presence of acetic anhydride at N termini, followed by cleavage in the presence of trifluoacetic acid and triisopropyl silane, water, and anisole as scavengers. Crude peptides were purified through a preparative reversed phase C-18 column on HPLC using water/acetonitrile with 2%/minute elution gradient. HPLC spectra and corresponding masspec spectra are shown in Supporting Information. Peptide **1**, expected mass $[M + H]^+$: 2502.8 Observed mass: 2502.4. Peptide **2**, expected mass $[M + Na]^+$: 2483.6 Observed mass: 2483.9. Peptide **3**, expected mass $[M + Na]^+$: 2527.7 Observed mass: 2528.3. Peptide **4**, expected mass $[M + Na]^+$: 2562.8 Observed mass: 2563.8.

Circular Dichroism. Spectra were acquired on a Jasco-J810 spectropolarimeter using a quartz cell with 1.0 mm path length for 50 μ M concentration, 0.1 mm path length for samples prepared at 0.1 wt% and 0.01 mm at 1 wt%. Spectra were collected at room temperature from 180 to 240 nm with a 0.2 nm interval at 50 nm/min. Millidegrees of rotation were converted to mean residual ellipticity. Samples were adjusted to the indicated pH by addition of HCl or NaOH as necessary.

FT-IR. Aliquots of peptide sample were deposited onto a diamond-ATR crystal (Specac "Golden Gate"), CaF₂ window, or gold mirror and air/nitrogen dried on the surface to form a thin layer of peptide nanofibers followed by examination using a Jasco FTIR 660plus. Grazing angle FT-IR spectra were recorded with an 80Spec specular reflectance accessory (PIKE Technologies). Collected spectra were linear baseline corrected and subsequently deconvoluted by fitting with a mixed Gaussian/Lorentzian using a least-squares method.

Cryo Transmission Electron Microscopy. Three microliters of sample were placed on a holy carbon grid and blotted for 2 s to generate a thin film. The samples were plunged into liquid ethane for quick freezing (Vitrobot type FP5350/60) and transferred to a cryo holder under the protection of liquid nitrogen. Samples were imaged on a JEOL 2010 microscope at -176 °C using low dose conditions. Samples were analyzed 1 h, 1 day, and 1 week after preparation. Regardless of the time point selected, samples displayed either no fibers (below 0.1% by weight) or fibers (at or above 0.1% by weight).

Sedimentation Equilibrium. The apparent molar mass and the dissociation constant of peptide **3** was determined in a Beckman Optical XL-A analytical ultracentrifuge equipped with a Ti60 titanium four-hole rotor with six-channel and 12 mm path length centerpiece. Equilibrium experiments were performed at 20 °C using three different concentrations (0.20, 0.39, 0.68 mM). Samples were run at three different rotor speeds: 50 000, 55 000, and 60 000 rpm. Loading volumes of sample and reference were 95 and 110 μ L, respectively. The sample was believed to be at equilibrium when the peptide distribution remained constant over two hours at a given rotor speed (typically 14 h of rotation). Data analysis was carried out using single-species model function and monomer-dimer

(24) Ryadnov, M. G.; Woolfson, D. N. *J. Am. Chem. Soc.* **2005**, *127*, 12407–12415.

(25) Dong, H.; Hartgerink, J. D. *Biomacromolecules* **2006**, *7*, 691–695.

(26) Dong, H.; Hartgerink, J. D. *Biomacromolecules* **2007**, *8*, 617–623.

(27) Harbury, P. B.; Zhang, T.; Kim, P. S.; Alber, T. *Science* **1993**, *262*, 1401–1407.

(28) Woolfson, D. N. *Adv. Protein Chem.* **2005**, *70*, 79–112.

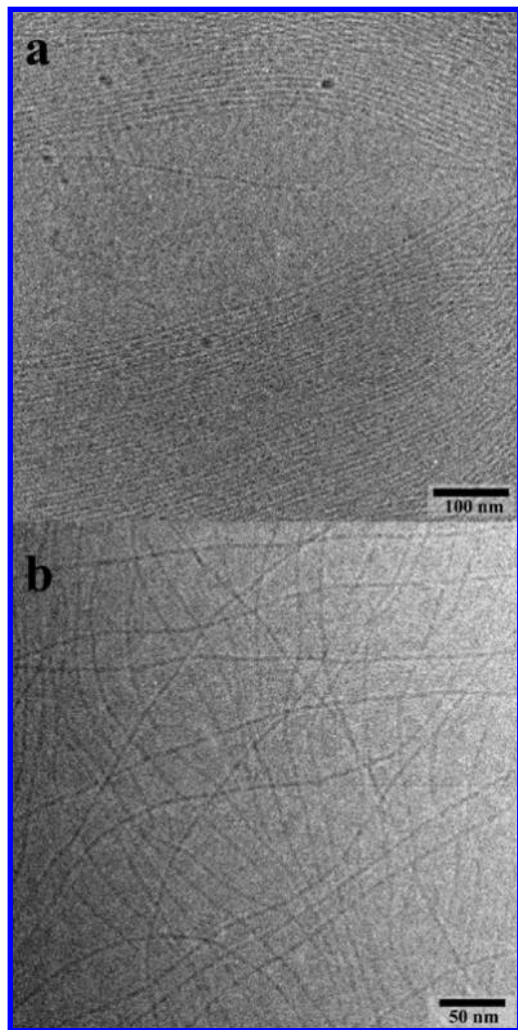


Figure 1. Cryo-TEM image of peptide **1** at (a) 1 wt% (4 mM) and pH 3.3 and (b) 0.1 wt% (0.4 mM) and pH 3.5.

equilibrium model function by nonlinear least-squares method provided by UltraScan software.

Results and Discussion

Peptides were induced to self-assemble by lowering the solution pH to 3.5, thereby neutralizing the glutamic acid side chains. The nanostructures resulting from the self-assembly process were examined by vitreous ice cryo-TEM. The secondary structure associated with the formation of nanostructures was examined by circular dichroism polarimetry (CD) and FT-IR. Although CD and FT-IR both showed α -helical secondary structure for peptide **1** at 0.1 wt% and 1 wt% (equal to 0.4 mM and 4 mM respectively) as characterized by the double minima at 208 and 222 nm in the CD spectrum and strong 1652 cm^{-1} absorbance in the IR spectrum (Figure SI-1, Supporting Information), the nanostructure revealed by TEM was significantly different between the two concentrations. As shown in Figure 1a and Figure SI-2, Supporting Information, cryo-TEM at 1 wt% revealed a hierarchical organization of bundles of fibrils with 4 nm diameter. Dilution of peptide **1** to 0.1 wt% resulted in fiber unbundling. At this lower concentration cryo-TEM showed individually isolated fibrils with diameters of 4 nm (Figure 1b). This indicates that the addition of positively charged amino acids in the peripheral region appears to have successfully prevented lateral aggregation or “ripening” of fibrils

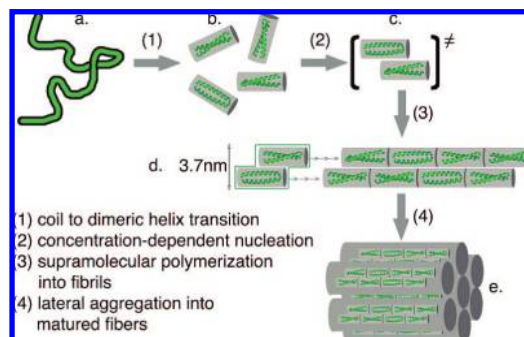


Figure 2. Proposed mechanism of self-assembly into nanofibers.

under diluted condition through electrostatic repulsion. When the concentration is below 0.1 wt%, no fibers of any kind could be observed (data not shown).

Assuming the nanofibrous structure observed at 0.1 wt% illustrates the minimal level of hierarchy in nanofiber organization, and because there are no design features in the primary sequence to promote sticky ended assembly, we propose an alternative mechanism for fiber formation. We propose that traditional blunt ended coiled coils are formed (Figure 2b) which above a minimum concentration associate with one another in an offset pair of coiled coils (Figure 2c). This serves as a nucleation point for fiber formation.

Such an organization allows the propagation of nanofibers in the axial direction without performing a sticky ended dimer dictated by peptide primary sequence and reflects an alternative way to generate coiled coil based nanofibers. In fact, the peptide tetramer composed of side by side packed coiled coil dimers has been previously observed by Kim et al.²⁹ in 2001 in a synthetic heterodimeric coiled coil. Their crystal structure indicated three copies of the dimer per asymmetric unit (protein data bank id: 1kd8, see Figure SI-12, Supporting Information for illustration). Two copies are in close contact with one another by means of noncovalent interaction between residues found both in the peripheral (positions *b*, *c*, *f*) and the electrostatic (positions *e*, *g*) regions, giving rise to an antiparallel association of dimeric coiled coils approximately 3.7 nm in diameter. This is in good agreement with the dimensions of coiled coil fibrils we have observed by cryo-TEM (4 nm, Figure 1). Figure 2d shows a cartoon of the minimum fibril structure with a 3.7 nm diameter.

It has been reported in the literature that α -helical fibers can be created both from α -helices oriented parallel to the fiber axis¹⁰ and α -helices oriented perpendicular to the fiber axis.³⁰ To differentiate these possibilities, we have performed oriented FT-IR measurements similar to those performed on other self-assembling peptide fibers.^{26,31–33} These results demonstrate conclusively that the fibers are composed of α -helices (amide I at 1652 cm^{-1}) and that these α -helices are oriented parallel to the fiber axis. (see supplementary Figure SI-11, Supporting Information).

(29) Keating, A. E.; Malashkevich, V. N.; Tidor, B.; Kim, P. S. *Proc. Natl. Acad. Sci. U.S.A.* **2001**, *98*, 14825–14830.

(30) Lazar, K. L.; Miller-Auer, H.; Getz, G. S.; Orgel, J. P. R. O.; Meredith, S. C. *Biochemistry* **2005**, *44*, 12681–12689.

(31) Kim, H. S.; Hartgerink, J. D.; Ghadiri, M. R. *J. Am. Chem. Soc.* **1998**, *120*, 4417–4424.

(32) Paramonov, S. E.; Jun, H. W.; Hartgerink, J. D. *J. Am. Chem. Soc.* **2006**, *128*, 7291–7298.

(33) Dong, H.; Paramonov, S. E.; Aulisa, L.; Bakota, E. L.; Hartgerink, J. D. *J. Am. Chem. Soc.* **2007**, *129*, 12468–12472.

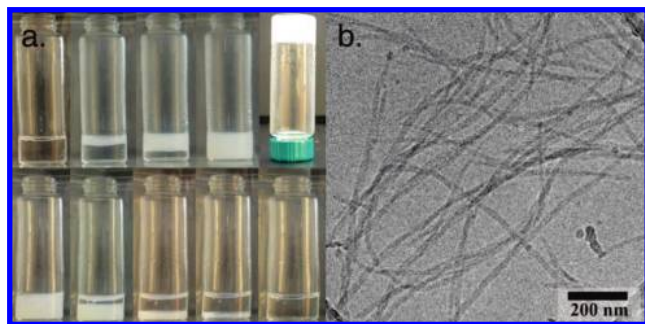


Figure 3. (a) Gel formation and dissolution with treatment of concentrated HCl and NH_4OH vapor. (Upper) from left to right, peptide **2** dissolved in water at a concentration of 1 wt% (4.065 mM) at pH 9 is exposed to HCl vapor. (Lower) Gel formed upon acidification is treated with ammonia hydroxide leading to fully dissolution. (b) Cryo-TEM image of nanofibers formed by gelated peptide **2**.

The key parameter controlling fiber formation in our system is concentration. Several samples of peptide **1** prepared at different concentration were examined by cryo-TEM and only when the concentration is above 0.1 wt% are fibers present. At high concentrations the small fibrils bundle into fibers with much larger diameter (Figure 2e). At lower concentration, equilibrium lies in favor of soluble, dimeric coiled coils. Although we are proposing an alternative mechanism of fiber formation, it should be noted that this is not in conflict with the sticky ended coiled coil mechanism proposed by Woolfson but simply shows an alternative route to fiber formation which may be applicable to a wide range of coiled coils at high concentrations. Fiber formation at lower concentration (for example 100 μM in contrast with 400 μM in our system) can be achieved in systems, such as the SAF peptides developed by Woolfson's group,¹⁰ in which sticky ends are designed to favor the elongation of nanofibers.

Additional peptides were synthesized and tested for their ability to form nanofibers as peptide concentration changes. As with peptide **1**, peptide **2** and **3** formed hydrogels at 1 wt% at acidic pH, where the glutamic acids are fully neutralized to avoid charge repulsion between adjacent helices. Figure 3a shows the reversible formation and dissolution of a self-supporting gel formed by peptide **2** (peptide **1** under the same condition formed transparent hydrogels which are difficult to photograph). Self-assembly was triggered by the addition of concentrated HCl vapor and disassembly was accomplished by neutralization with ammonium hydroxide. The gels were examined by vitreous ice cryo-TEM revealing formation of large quantities of fibers with ~ 20 nm diameter, as shown in Figure 3b.

Gel samples were deposited and dried onto a diamond surface and examined by attenuated total reflection (ATR) FT-IR to identify the secondary structure involved in the formation of self-assembled nanofibers. As shown in Figure SI-3, Supporting Information, a major peak at 1650 cm^{-1} appeared in amide I band for peptide **2**, indicating the presence of α helical secondary structure as opposed to β sheets or random coils. CD (Figure SI-4, Supporting Information) also revealed a spectrum characteristic of α helical organization with double minima at 208 and 222 nm, respectively. At low concentration, the helical structure remains, but fibers do not form (Figure SI-7, Supporting Information). For peptide **2**, only thick fiber bundles were observed even at a concentration at which peptide **1** forms very thin fibers. The diameter of these fibers is much larger than what we expect for two units of coiled coil dimers. These large 20 nm bundles are likely due to lateral association

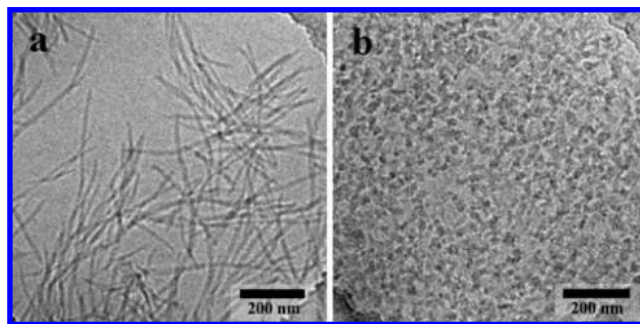


Figure 4. Cryo-TEM image of (a) peptide **3** and (b) peptide **4** at 1 wt% (3.995 mM for peptide **3** and 3.938 mM for peptide **4**) and pH 3.3.

of individual coiled coil fibrils, similar to previously reported systems^{10,13,18,34} where nanofibers built from coiled coil peptides were shown to aggregate into thicker fibers in a 3D hexagonal lattice.³⁵ We believe fiber ripening, in our case, is a process facilitated by the noncovalent interactions between hydrophilic residues (glutamine and serine) occupying peripheral positions and/or neutralized glutamic acid from the electrostatic region between neighboring fibrils. Whereas in the case of peptide **1**, at 0.1% by weight, fibrils are limited to a 4 nm diameter due to the charge repulsion between lysine residues in the *b*, *c*, or *f* positions. The distinction in fiber bundling seen with peptide **1** and peptide **2** indicates the critical importance of residues in the peripheral region in controlling the nanoarchitecture of coiled coil nanofibers.

It has been demonstrated that peptides forming β -sheets exhibit similar fiber morphologies as shown in Figure 1.^{33,36} Furthermore, α -helical peptides have been shown to convert to β -sheet nanofibers over time or under adverse conditions.^{25,26} To exclude the possibility of β sheet formation in the self-assembly and fibril formation, extensive studies focusing on secondary structures as observed by CD and IR have been carried out to exclude β -sheet nanofiber formation across a wide concentration range (0.1 wt% - 1 wt%). In previous studies, β -sheet formation has been shown to be accelerated by increased concentration, long time of incubation and high temperature. To stress test, peptide **1** at 1 wt% was subject to 95 °C for half an hour before being cooled down to room temperature. CD showed unfolding at high temperature and refolding to α -helix (with no observable β -sheet formation) when the temperature was lowered (Figure SI-8c and SI-8d, Supporting Information). FT-IR spectra were then acquired after drying onto a diamond surface. Both nonheated and heated samples indicated α -helices as the predominant species (Figure SI-8a, Supporting Information). Similar heating and drying experiments were performed on peptide **2** (SI-8b) which also found no formation of β -sheet. An alternative explanation is that a soluble fraction of the peptide suspension was contributing to the α -helical signal and masking an underlying β -sheet signal. To eliminate this possibility the gel formed by peptide **2** was centrifuged at 13 000g for 8 min separating it into a fully soluble and clear supernatant and a white pellet. These were then examined separately by CD, FT-IR and cryo-TEM to characterize each fraction. As indicated

(34) Melnik, T. N.; Villard, V.; Vasiliev, V.; Corradin, G.; Kajava, A. V.; Potekhin, S. A. *Protein Eng.* **2003**, *16*, 1125–1130.

(35) Papapostolou, D.; Smith, A. M.; Atkins, E. D. T.; Oliver, S. J.; Ryadnov, M. G.; Serpell, L. C.; Woolfson, D. N. *Proc. Natl. Acad. Sci. U.S.A.* **2007**, *104*, 10853–10858.

(36) Lamm, M. S.; Rajagopal, K.; Schneider, J. P.; Pochan, D. J. *J. Am. Chem. Soc.* **2005**, *127*, 16692–16770.

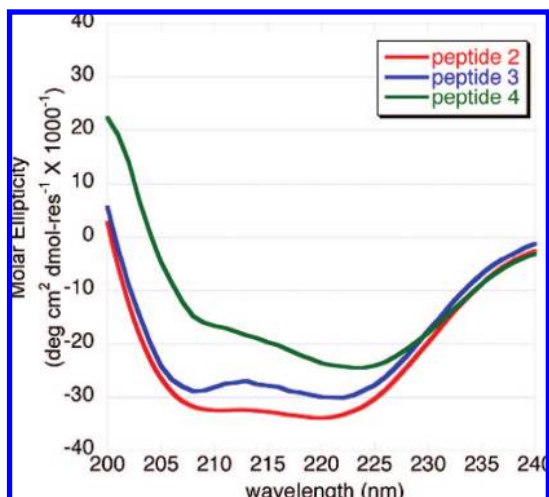


Figure 5. CD spectra of peptides **2**, **3**, and **4** at pH 4 and 0.1 wt% (0.407, 0.4, and 0.394 mM for peptides **1**, **2**, and **3**, respectively).

by the CD and IR data (Figure SI-5, Supporting Information), both the supernatant and the pellet consist of α -helices. Cryo-TEM of the soluble supernatant shows no fibrous structure, whereas the pellet displays aggregated fibrous structures similar to those seen in Figure 3b (Figure SI-6, Supporting Information). Combining the results from CD, IR, and cryo-TEM analysis, we believe these peptides form stable α -helices which self-assemble into fibrous structures when initiated by the appropriate stimuli (pH and concentration in this case) and that this secondary structure remains intact under all relevant conditions.

To promote the formation of coiled coil nanofibers as well as to keep the continuity of elongated fiber, peptides are required to be in a dimeric α -helical coiled coil conformation based on the mechanism proposed above. Any helix inhibitor should reduce fiber length or eliminate fiber formation altogether. To test this, peptide **3** and **4** were synthesized with the incorporation of tyrosine (Y) at *f* positions. The presence of tyrosine also allows analytical ultracentrifugation (AUC) to be performed. The AUC experiment was performed in acetate buffer at three different peptide concentrations (200, 390, and 680 μ M). A global fit to a single component allowed the determination of the apparent molecular weight, which was found to be 5369, indicating the presence of a coiled coil dimer. A global fit to a

dimer-equilibrium model allowed for the determination of the dissociation constant, which was found to be 12 μ M (Figure SI-10, Supporting Information), comparable to that of the dimerization domain of GCN4 ($K_d = 2.5 \mu$ M).³⁷

In addition to being a spectroscopic probe, tyrosine also has low helix propensity and as expected, peptide **3** with single tyrosine display fibers with significantly shortened length (Figure 4a). Incorporation of a second tyrosine in peptide **4** eliminates fiber formation. In fact, inspection of peptide **4** by cryo-TEM revealed only amorphous aggregation (Figure 4b) rather than the nanostructured fibers seen with peptides **1** - **3**. The reduced nanofiber length after inclusion of tyrosine indicates the low tolerance of fiber integrity to helix destabilization. Comparisons of the initial helicity of peptides **2**, **3**, and **4** show a good correlation of fiber length and CD at 222 nm (Figure 5). Direct comparison of peptides **2-4** with **1** cannot be made due to the electrostatic repulsion at acidic pH experienced by this peptide at pH 3.5.

Conclusion

We have described an alternative mechanism by which coiled coil peptides form nanofibers. The building blocks are composed of two units of coiled coil dimers arranged out of register with one another. The formation of high aspect ratio nanofibers driven by increased peptide concentration was found to be a generic effect for coiled coil peptides lacking design criteria necessary to form sticky-ended dimers. Narrow fibers diameters can be prepared when lateral aggregation is inhibited through incorporation of charged amino acids in the peripheral positions of a coiled coil. Additionally, fiber length can be modified by the inclusion of amino acids with reduced helical propensities.

Acknowledgment. This work was funded by The Robert A. Welch Foundation research grant C1557 and NSF CAREER Award DMR-0645474.

Supporting Information Available: Additional characterization of these peptides by HPLC, MS, CD, FT-IR, Cryo-TEM, and AUC is available. This information is available free of charge via the Internet at <http://pubs.acs.org/>.

JA8037323

(37) Wendt, H.; Berger, C.; Baici, A.; Thomas, R. M.; Bosshard, H. R. *Biochemistry* **1995**, *34*, 4097–4107.